SWI/SNF remains localized to chromatin in the presence of SCHLAP1

Jesse R. Raab[1], Keriayn N. Smith[1], Camarie C. Spear[1], Carl J. Manner[1], J. Mauro Calabrese[2] and Terry Magnuson [ID][1,3]*

SCHLAP1 is a long noncoding RNA that is reported to function by depleting the SWI/SNF complex from the genome. We investigated the hypothesis that SCHLAP1 affects only specific compositions of SWI/SNF. Using several assays, we found that SWI/SNF is not depleted from the genome by SCHLAP1 and that SWI/SNF is associated with many coding and noncoding RNAs, suggesting that SCHLAP1 may function in a SWI/SNF-independent manner.

The long noncoding RNA (lncRNA) second chromosome locus associated with prostate cancer 1 (SCHLAP1) is a promising biomarker for metastatic prostate cancer[1,2]. SCHLAP1 is proposed to function by antagonizing the SWI/SNF complex through direct interaction, leading to complete disruption of SWI/SNF genomic occupancy[1]. Evidence for this mechanism comes from the reported loss of SMARCB1 occupancy measured by chromatin immunoprecipitation followed by sequencing (ChIP–seq)[1]. SWI/SNF is a large multi-subunit chromatin remodeling complex that can be combinatorially assembled to yield hundreds to thousands of biochemically unique complexes[3–5]. We investigated the alternative hypothesis that distinct forms of SWI/SNF are affected by SCHLAP1 expression. However, using a varriety of biochemical and genomics assays, we demonstrate that SWI/SNF occupancy is unaffected by SCHLAP1 expression, in contrast to results reported previously[1]. We show that SWI/SNF binds coding and noncoding RNA, raising the possibility that SCHLAP1 function is SWI/SNF-independent.

Consistent with the report by Prensner et al.[1], we observed an interaction between SMARCB1 and SCHLAP1 (Fig. 1a). We next generated SCHLAP1-overexpressing benign prostate epithelial cells (RWPE1;SCHLAP1 cells) or control cells (RWPE1;*LACZ* cells)[1] (SCHLAP1 gift of A. Chinnaiyan). This model is the same as that originally used to suggest global depletion of SMARCB1 by SCHLAP1 (ref. [1]). We then confirmed the phenotype of the cells with respect to SWI/SNF expression and growth (Fig. 1b and Supplementary Figs. 1,2). In addition, we confirmed the key result that SCHLAP1 increased cell invasion (Fig. 1c).

To investigate which SWI/SNF subunits were depleted from chromatin upon SCHLAP1 expression, we fractionated RWPE1;*LACZ* and RWPE1;SCHLAP1 cells based on subcellular localization or salt extraction. Surprisingly, all SWI/SNF subunits assayed remained strongly enriched in the chromatin or high salt fractions (Fig. 1d and Supplementary Figs. 3–5). Consistent with these biochemical experiments, we found that SMARCA4 and SMARCB1 localization was not affected in RWPE1;SCHLAP1 cells by immunofluorescence (Supplementary Fig. 3b). Immunoprecipitation of SMARCA4 or SMARCB1 demonstrated that the SWI/SNF complex remains intact

in the presence of SCHLAP1 (Supplementary Figs. 3c,6). Finally, we used a malignant rhabdoid tumor cell line with inducible SMARCB1 that, when expressed, causes growth arrest (gift of B. Weissman)[6]. We reasoned that, if SCHLAP1 disrupted SMARCB1 chromatin occupancy, then overexpression of SCHLAP1 should allow G401 cells to proliferate following induction of SMARCB1. However, SMARCB1 induction led to growth arrest in a dose-dependent manner (Fig. 1e and Supplementary Figs. 7,8). Together, these results demonstrate that SCHLAP1 does not induce changes to SWI/SNF composition or its association with chromatin.

We next performed ChIP–seq for three SWI/SNF subunits (SMARCB1, SMARCA2, and SMARCA4) in RWPE1;SCHLAP1 cells. In contrast to a previous report[1], we identify robust binding for all three subunits in RWPE1 cells expressing SCHLAP1 (Fig. 1f). In RWPE1;SCHLAP1 cells, we identified 6,490, 22,185, and 51,505 peaks for SMARCB1, SMARCA2, and SMARCA4, respectively (Supplementary Table 1). This large number of peaks is in contrast to the previous report[1], which identified approximately 6,500 SMARCB1 peaks in RWPE1;*LACZ* cells and close to no peaks in the SCHLAP1-expressing cells. The numbers of peaks are consistent with previous work from our laboratory, which showed 30,000–45,000 SMARCA4 peaks[4]. In addition, we and others have reported a large number of SWI/SNF peaks for a variety of subunits[3,4,7,8]. The majority of SMARCA2 peaks overlapped a SMARCA4 peak (Supplementary Fig. 9a), and SWI/SNF peaks were predominantly located at promoters (45–75%; Supplementary Fig. 9b)[4]. SWI/SNF binding was most prominent at highly expressed genes, with little to no occupancy at non-expressed genes (Fig. 1g; expression data from GSE98898 (ref. [9])). These results demonstrate that SCHLAP1 does not function by disrupting SWI/SNF occupancy genome-wide, and raises the question of how SCHLAP1 functions to promote cell invasion and progression to metastatic disease.

To investigate whether SCHLAP1 expression induces chromatin changes, we performed assay for transposase-accessible chromatin with high-throughput sequencing (ATAC-seq) on RWPE1;*LACZ* and RWPE1;SCHLAP1 cells[10]. We identified 273 and 3,167 sites that open and close, respectively (Supplementary Table 2 and Supplementary Fig. 10). The sites that open were more likely to be located distally or in introns of genes (Supplementary Fig. 10). Sites that open upon SCHLAP1 expression were enriched for distinct motifs compared to those that close (Supplementary Fig. 11 and Supplementary Tables 3, 4). Open sites were enriched in motifs for TEAD and AP1 transcription factors, which are known to have a role in defining oncogenic enhancers (Supplementary Fig. 11 and Supplementary Tables 3, 4)[11]. To test whether these sites became

[1]Department of Genetics, University of North Carolina at Chapel Hill, Chapel Hill, NC, USA. [2]Department of Pharmacology and Lineberger Comprehensive Cancer Center, University of North Carolina, Chapel Hill, NC, USA. [3]Lineberger Comprehensive Cancer Center, University of North Carolina at Chapel Hill, Chapel Hill, NC, USA. *e-mail: tmagnuson@unc.edu
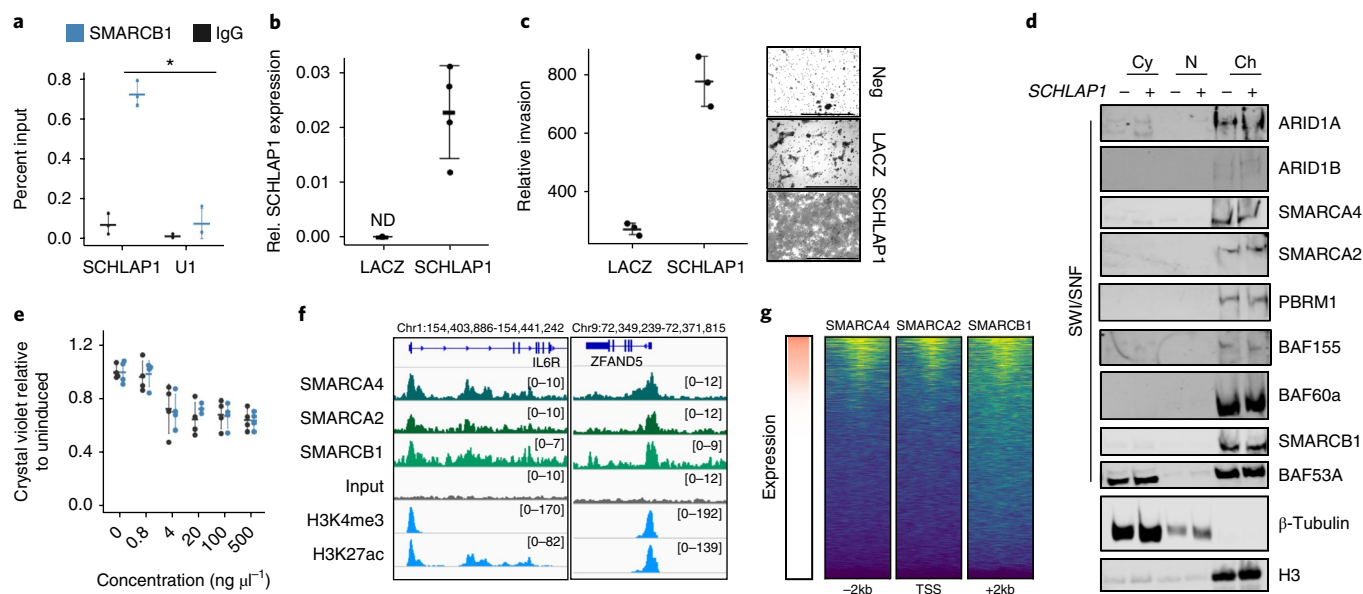
Fig. 1 | SCHLAP1 does not evict SWI/SNF from chromatin. a, Native RIP for SMARCB1. *$P = 0.02$ (two-sided *t*-test) for SCHLAP1 versus U1 primer sets for SMARCB1 immunoprecipitation. $n = 3$ independent experiments. Error bars represent the mean, and whiskers represent the standard deviation. **b**, SCHLAP1 expression in RWPE1;*LACZ* and RWPE1;SCHLAP1 cells relative to *GAPDH*. $n = 3$ independent cell lines. Error bars represent mean and standard deviation. ND, not detected. **c**, Invasion assay of RWPE1;*LACZ* and RWPE1;SCHLAP1 cells using fluorescent intensity (Licor). Representative of $n = 3$ independent invasion assays run on one cell line, $P = 0.007$ (two-sided *t*-test). Error bars represent mean and standard deviation. Scales bars, 500 uM. **d**, Chromatin fractionation showing SWI/SNF subunit presence in cytoplasm (Cy), nuclear (N), or chromatin (Ch) fractions from RWPE1;*LACZ* and RWPE1;SCHLAP1 cells. Representative images from two independent experiments. **e**, Quantitation of G401 growth inhibition. $n = 4$, two independent cell lines plated in duplicate, error bars equal mean ± standard deviation. **f**, Example browser images for SMARCA4, SMARCA2, and SMARCB1 from RWPE1;SCHLAP1 cell ChIP–seq experiments. Aggregate data from two independent ChIP–seq experiments are shown. **g**, Occupancy for SMARCA4, SMARCA2, and SMARCB1, centered on all transcription start sites (GENCODE), aligned by expression in RWPE1 cells. $n = 57,662$.

activated enhancers, we performed ChIP–seq for H3K4me1, H3K4me3, and H3K27ac in RWPE1;*LACZ* and RWPE1;SCHLAP1 cells (Supplementary Fig. 10b), but we did not find differences in any histone modifications. In addition, SMARCA2, SMARCA4, and SMARCB1 remained highly enriched on sites that decrease chromatin openness (Supplementary Fig. 10d). Gene ontology analysis of the open sites identified pathways involved in responses to nuclear factor-κB (NF-κB) signaling, epithelial to mesenchymal transitions, and nucleotide metabolism (Supplementary Fig. 11b), whereas closed sites were enriched for pathways involved in cell adhesion and signal transduction (Supplementary Fig. 11b). Although we noted changes in gene expression associated with ATAC-seq changes, we did not detect a significant association with the direction of altered chromatin openness (Supplementary Fig. 12)[1]. These data suggest that SCHLAP1 could modestly influence chromatin, but is not sufficient to induce histone modification changes.

Recent evidence suggests that chromatin regulators display widespread interactions with RNA[12–17]. Therefore, we investigated whether SWI/SNF interacts with other lncRNA using crosslinked RNA immunoprecipitation and sequencing (RIP-seq) for SMARCA4 and a general splicing factor (SFPQ) as a control (Fig. 2a,b)[18]. Consistent with previous observations of chromatin regulators, we saw widespread enrichment of SMARCA4 on most expressed transcripts relative to an immunoglobulin-G (IgG) control (Supplementary Tables 5,6)[18]. Hendrickson et al.[18] used the same formaldehyde RIP-seq (fRIP-seq) to demonstrate that chromatin regulators could display either exonic or intronic enrichment. The pattern of SWI/SNF enrichment seemed to be uniform throughout the transcript, suggesting that SMARCA4 associates frequently with primary transcripts (Fig. 2c–f). In contrast, SFPQ was mostly enriched at exons and showed high levels of enrichment at the 3′ UTR of many transcripts. We observed SMARCA4 and SFPQ signal at SCHLAP1,

although the level of enrichment was not markedly different between the proteins. Among the enriched transcripts was *NEAT1*, which is a known interacting partner of both SWI/SNF[13] and SFPQ[19–21]. In addition, we identified high levels of SMARCA4 associated with MALAT1, whereas SFPQ was not enriched (Fig. 2a,b). A recent report showed a functional interaction between SMARCA4, HDAC9, and MALAT1, further supporting the specificity of our result[17]. Given the widespread binding of SMARCA4 on many RNAs, and the modest enrichment of SCHLAP1 relative to bona fide SWI/SNF interactions such as MALAT1, we interpret these data as evidence that the SCHLAP1–SWI/SNF interaction is the result of a widespread nonspecific interaction between SWI/SNF and transcribing RNA. This may be functional as RNA has been shown to inhibit activity of SWI/SNF and PRC2 (refs [16,22]).

Together, these results demonstrate that the interaction between SWI/SNF and SCHLAP1 does not lead to a global depletion of SWI/SNF from the genome as reported previously[1]. We confirm that SCHLAP1 induces RWPE1 cells to become more invasive, and our results suggest that this phenotype may be driven by a SWI/SNF-independent mechanism.

Online content

Any methods, additional references, Nature Research reporting summaries, source data, statements of data availability and associated accession codes are available at https://doi.org/10.1038/s41588-018-0272-z.

References
1. Prensner, J. R. et al. *Nat. Genet.* **45**, 1392–1398 (2013).

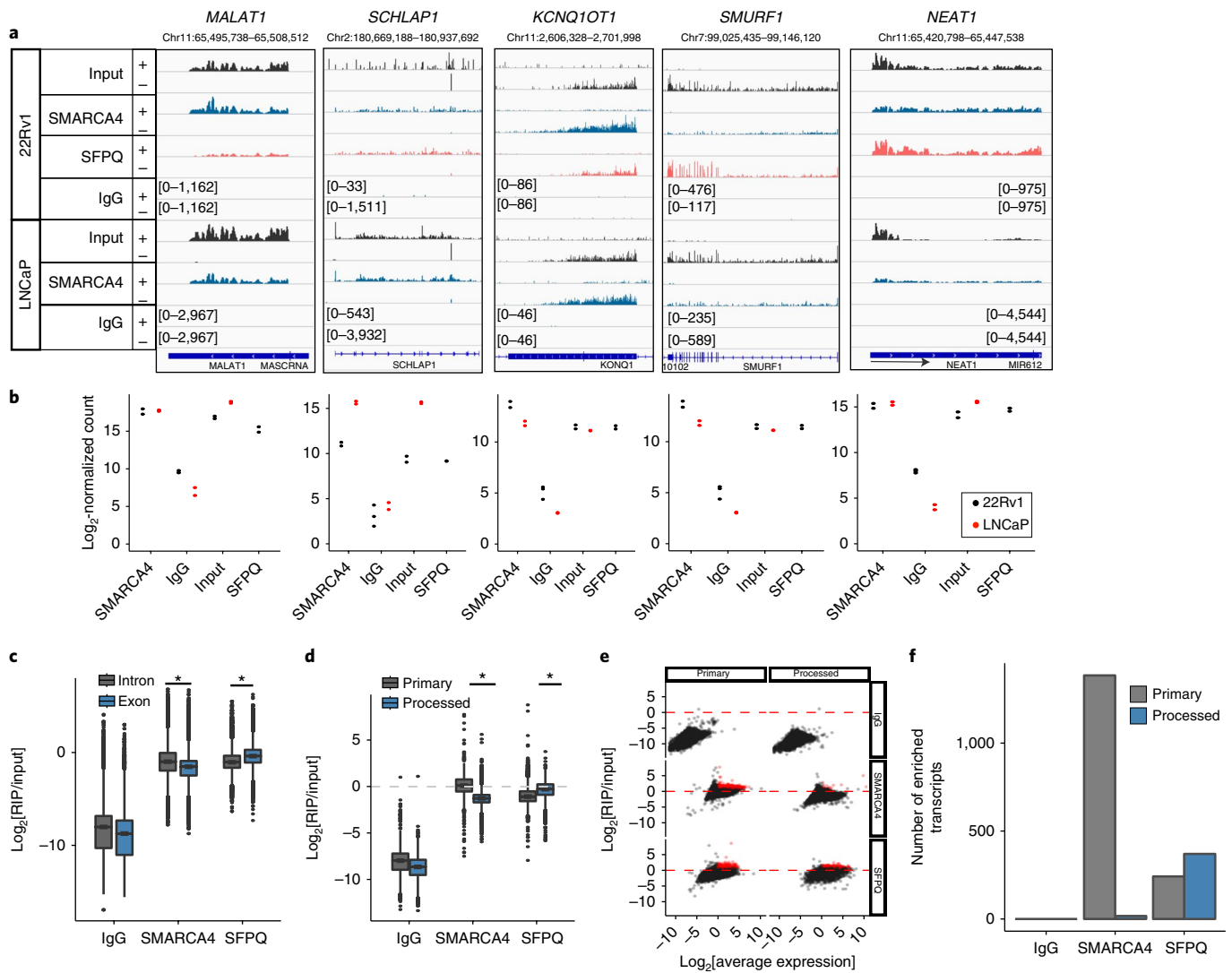**Fig. 2 | SMARCA4 binds many RNAs. a**, Example loci associated with SMARCA4 or SFPQ in 22Rv1 and LNCaP cells. Reads mapping to the forward (+) and reverse (−) strand for each locus are shown. Within cell lines and on the same strand, scales are equal. RIP-seq was performed two times for each antibody in each cell line. Arrow in *NEAT1* panel denotes a smaller transcript within the longer *NEAT1* transcript. **b**, Quantitation of signal at each of the genes in **a** for each antibody and each cell line. **c**, Enrichment of reads mapping to exons compared to introns for each immunoprecipitate. $*P < 2.2 \times 10^{-16}$, Wilcoxon test. Boxplots show the first, second, and third quartile, and whiskers extend to 1.5 times the interquartile range. **d**, Enrichment of reads mapping to primary compared to processed transcripts. $*P < 2.2 \times 10^{-16}$ for both tests, two-sided wilcoxon test. Boxplots show the first, second, and third quartile, and whiskers extend to 1.5 times the interquartile range. **e**, Log_2 fold change relative to input is plotted against the average expression of a transcript for both the primary and processed transcripts for the three antibodies tested. Red dots indicate genes with a $\log_2$ fold change of greater than 1 and an average $\log_2$ fold change of greater than 0. **f**, Number of transcripts assigned to the red points in **e**.

2. Prensner, J. R. et al. *Lancet Oncol.* **15**, 1469–1480 (2014).
3. Raab, J. R., Resnick, S. & Magnuson, T. *PLoS Genet.* **11**, e1005748 (2015).
4. Raab, J. R., Runge, J. S., Spear, C. C. & Magnuson, T. *Epigenetics Chromatin* **10**, 62 (2017).
5. Kadoch, C. & Crabtree, G. R. *Cell* **153**, 71–85 (2013).
6. Kuwahara, Y., Wei, D., Durand, J. & Weissman, B. E. *Mol. Cancer Res.* **11**, 251–260 (2013).
7. Morris, S. A. et al. *Nat. Struct. Mol. Biol.* **21**, 73–81 (2014).
8. Nakayama, R. T. et al. *Nat. Genet.* **49**, 1613–1623 (2017).
9. Luo, Z., Rhie, S. K., Lay, F. D. & Farnham, P. *Cell Rep.* **21**, 1411–1417 (2017).
10. Buenrostro, J. D., Giresi, P. G., Zaba, L. C., Chang, H. Y. & Greenleaf, W. J. *Nat. Methods* **10**, 1213–1218 (2013).
11. Zanconato, F. et al. *Nat. Cell Biol.* **17**, 1218–1227 (2015).
12. Cheng, S., Wang, L., Deng, C.-H., Du, S.-C. & Han, Z.-G. *Biochem. Biophys. Res. Commun.* **491**, 178–182 (2017).
13. Kawaguchi, T. et al. *Proc. Natl Acad. Sci. USA* **112**, 4304–4309 (2015).
14. Wang, Y. et al. *Cell Stem Cell* **16**, 413–425 (2015).
15. Zhu, Y., Rowley, M. J., Böhmdorfer, G. & Wierzbicki, A. T. *Mol. Cell* **49**, 298–309 (2013).
16. Cajigas, I. et al. *Development* **142**, 2641–2652 (2015).
17. Lino Cardenas, C. L. et al. *Nat. Commun.* **9**, 1009 (2018).
18. Hendrickson, D. G., Kelley, D. R., Tenen, D., Bernstein, B. & Rinn, J. L. *Genome. Biol.* **17**, 28 (2016).
19. Clemson, C. M. et al. *Mol. Cell* **33**, 717–726 (2009).
20. Hirose, T. et al. *Mol. Biol. Cell.* **25**, 169–183 (2014).
21. Naganuma, T. et al. *EMBO J.* **31**, 4020–4034 (2012).
22. Kaneko, S., Son, J., Shen, S. S., Reinberg, D. & Bonasio, R. *Nat. Struct. Mol. Biol.* **20**, 1258–1264 (2013).

Acknowledgements

Competing interests

The authors declare no competing interests.

Additional information

Supplementary information is available for this paper at https://doi.org/10.1038/s41588-018-0272-z.

Reprints and permissions information is available at www.nature.com/reprints.

Correspondence and requests for materials should be addressed to T.M.

Publisher's note: Springer Nature remains neutral with regard to jurisdictional claims in published maps and institutional affiliations.

Methods

Cell culture. RWPE1 cells were purchased from the American Type Culture Collection (ATCC) (CRL-11609, lot 61840713) and grown in Keratinocyte Serum Free Medium (Life Technologies) supplemented with penicillin and streptomycin. Cells were short-tandem repeat (STR) profiled by ATCC before purchase, and all experiments were performed on low-passage cells (<10 passages). Lenti6-*LACZ* was generated by removing *SCHLAP1* from the plasmid below and cloning *LACZ* from pLentipuro-*LACZ* into pLenti6 from which *SCHLAP1* was removed by EcoRI-BamHI digest. Lenti6-*SCHLAP1* was a gift of A. Chinnaiyan[1]. Lentiviral particles were produced using psPAX2 and pMD2.G to package plasmids in 293 T cells. RWPE1;*LACZ* and RWPE1;SCHLAP1 cells were then generated by transduction with lentivirus and selecting with 2.5 µg ml⁻¹ blasticidin for 1 week. 22RV1 and LNCaP cells were purchased from ATCC (CRL-2505, lot 60437301; CRL-1740, lot 62129998) and grown in RPMI 1640 with 10% fetal bovine serum FBS solution supplemented with penicillin and streptomycin. Cells were STR profiled by ATCC prior to purchase and were used at early passages (<10 passages). All cells were tested for (and found to be free of) mycoplasma contamination.

Antibodies. SMARCA2 (Cell Signaling 11966), lot 2; SMARCA4 (Abcam ab110641), GR150844-42; SMARCB1 (Abcam ab192864), GR315927-2; BAF53A (Abcam ab3882), GR95633-1; BAF60A (BD Biosciences 611728), 5199785; BAF155 (Cell Signaling D7F8S), lot 2; BAF180 (Bethyl A301-591A), lot 1; SFPQ (Genetex GTX114209), 40828; NCL (Bethyl A300-711A), lot 1; ARID1A (Abcam ab182560), GR3186289-2; ARID1B (Abcam ab57461), GR308911-3; ARID2 (ThermoFisher PA5-35857), SF24034426; H3K4me3 (Abcam ab8580); H3K4me1 (Active Motif 39635), 16611004; H3K27ac (Active Motif 39133), 20017049; H3 (epicypher 13-0001), gift of B. Strahl, available from Epicypher.

Invasion assay. Invasion was assessed using a Corning BioCoat Matrigel Invasion Assay with an 8-µm pore size. Cells were seeded into Boyden chambers at 100,000 cells per well in 100 µl of normal growth medium. The lower chamber was filled with either normal growth medium supplemented with 10% FBS or PBS solution as a negative control. Cells were allowed to invade for 40.25 h, after which the top chamber was swabbed to remove non-invading cells. Invading cells were fixed and stained with crystal violet. Membranes were imaged using a Zeiss Axio Imager for representative images or scanned using a Licor fluorescent imager for quantitation. Results are reported as the average of three biological replicates. For each replicate, crystal violet fluorescence was measured and background fluorescence was subtracted. Background fluorescence of the membranes was obtained from a negative control.

RNA immunoprecipitation. RIP experiments were performed using a modified version of a protocol from Hendrickson et al.[18].

Fixation. 22Rv1 and LNCaP cells were fixed in 0.3% methanol-free formaldehyde for 30 min at 4 °C. Formaldehyde was quenched with 125 mM glycine for 5 min at 20–25 °C. Plates were washed three times in PBS at 20–25 °C, and cells were scraped in 1 mM PMSF (phenylmethyl sulfonyl fluoride) in PBS. Cells were snap frozen in liquid nitrogen and stored at −80 °C.

Fragmentation and immunoprecipitation. Cells were resuspended in 0.5 ml radioimmunoprecipitation assay (RIPA) buffer (50 mM Tris-HCl pH 8, 1% Triton X-100, 0.5% sodium deoxycholate, 0.1% SDS, 5 mM EDTA, 150 mM KCl) plus 0.5 mM DTT with 1× protease inhibitors (Sigma) and 2.5 µl RNAsin, and incubated on ice for 10 min prior to lysing using a Bioruptor (Diagenode) for two cycles of 30 s on and 1 min off, followed by centrifugation at 4 °C for 10 min at maximum speed. Protein A magnetic beads (Biorad) were pre-conjugated with antibody for 2 h at 4 °C. Cells were then incubated overnight at 4 °C with antibody-conjugated beads. Beads were washed consecutively with fRIP buffer (25 mM Trix-HCl pH 7.5, 5 mM EDTA, 0.5% Ipegal CA-630, 150 mM KCl), three times in ChIP buffer (50 mM Tris-HCl pH 7.5, 140 mM NaCl, 1 mM EDTA, 1 mM EGTA, 1% Triton X-100, 0.1% sodium deoxycholate, 0.1% SDS), 1× in high salt buffer (ChIP buffer, but with 500 mM NaCl) and 1× in fRIP buffer. All washes were performed for 5 min at 4 °C. After the final wash, beads were resuspended in 56 µl water and 33 µl of 3× reverse crosslinking buffer (3× PBS, 6% N-lauroyl sarcosine, 30 mM EDTA) supplemented with 5 mM DTT. We then added 20 µl proteinase K and 1 µl RNAsin and incubated 1 h at 42 °C, 1 h at 55 °C, and 30 min at 65 °C. Following elution and crosslink reversal, Trizol was used to extract RNA. Finally, RNA in the aqueous phase was supplemented with 1 volume of ethanol and purified using a Zymo-spin IC column, including the on-column DNase digestion, as per the manufacturer's instruction. RNA was eluted in 15 µl double distilled water (ddH₂0) and used to prepare RNA-seq libraries or to synthesize cDNA for quantitative PCR. RNA-seq libraries were prepared by using equal volumes of immunoprecipitates and included 1 µl of 1:250 µl dilution of ERCC spike-in mix 1 (Life Technologies). Input libraries were prepared from the same amount of RNA as the immunoprecipitate with the most RNA, and spike-ins were added as above. Libraries were then prepared using the Kapa Ribo-zero kit following the manufacturer's instructions, pooled, and sequenced using single-end 75-bp reads on an Illumina Nextseq 500.

RIP-seq analysis. Reads were aligned, using STAR, to hg38 with GENCODE version 27 (v27) annotations that included ERCC spike-ins and using --quantMode GeneCounts. In parallel, an alignment-free quantitation method (Salmon version 0.8) was used to quantitate GENCODE v27 transcripts containing ERCC spike-ins and an extra transcript for each gene that contained the whole genomic DNA locus to represent an unspliced transcript. Browser tracks were generated by converting BAM files to bigWig files using Deeptools (version 2.5.2) and scaling tracks relative to the 75th percentile of the ERCC spike-ins. Enrichment of the immunoprecipitate relative to IgG was calculated using DESeq2 (v1.18.1) with sizeFactors generated from only the ERCC spike-in data. For visualization relative to input, normalized count values were used, and $\log_2$[RIP/input] was calculated for each gene. RIP-seq data are available under GEO accession GSE114393.

Chromatin fractionation. Chromatin fractionation was performed as described previously[23]. Approximately 1×10^7 cells were washed and resuspended in 200 µl Buffer A (10 mM HEPES pH 7.9, 10 mM KCl, 1.5 mM MgCl₂, 0.34 M sucrose, 10% glycerol, 1 mM DTT, supplemented with 1× protease inhibitors and 1 mM PMSF). Triton X-100 was then added to 0.1% final concentration, and cells were incubated for 8 min on ice. Cells were centrifuged at 1,300 g for 5 min at 4 °C. The supernatant was saved as the cytosolic fraction and the pellet (nuclei) was washed once with Buffer A. Cells were lysed for 30 min on ice in 100 µl Buffer B (3 mM EDTA, 0.2 mM EGTA, 1 mM DTT) supplemented with 1× protease inhibitors and 1 mM PMSF, and centrifuged at 1,700 g for 5 min at 4 °C. The supernatant was saved as the nucleoplasmic fraction, and the insoluble material was resuspended in 1× Laemmli buffer, and sonicated twice for 30 s on high power (Bioruptor). All lysates were boiled for 10 min in 1× Laemmli buffer with 0.1 M DTT and used in western blot analysis.

Salt extraction of nuclei. Salt extraction of chromatin was performed as described previously[24]. Cells were collected from plates prior to the protocol, snap frozen on liquid nitrogen and stored at −80 °C prior to extraction. Frozen cells were thawed on ice and resuspended gently 1 ml hypotonic buffer (10 mM HEPES pH 7.9, 1.5 mM MgCl₂, 10 mM KCl, 1 mM PMSF, 0.5 mM DTT) and incubated for 30 min on ice, then homogenized using a Dounce 40 times with a tight pestle, after which an aliquot was set aside as whole-cell extract. Cells were spun at 1,500 g for 5 min and the supernatant removed. Next, 400 µl of Buffer III.A (10 mM Tris pH 7.4, 2 mM MgCl₂, 1 mM PMSF, 5 mM CaCl₂) was added gently with a wide-orifice p1000 tip and 1 µl MNase (New England Biolabs, 2,000 U) was added. Nuclei were incubated for 30 min at 37 °C in a water bath, mixing every 10 min. To stop MNase digestion, 25 µl of ice-cold 0.1 M EGTA was added to nuclei and an aliquot was set aside as the nuclei fraction. Nuclei were then centrifuged at 400 g for 10 min at 4 °C and the supernatant was kept as the MNase fraction. Nuclei were then washed with 400 µl Buffer III.B (same as Buffer III.A, but without CaCl₂). Chromatin fractions were isolated by adding 400 µl of IV.80, incubating for 30 min and spinning as above. The supernatant following each spin was saved, and the next salt buffer was added (IV.80, IV.150, IV.300, IV.600, 10 mM Tris pH 7.4, 2 mM MgCl₂, 2 mM EGTA, 0.1% Triton X-100, with the amount of NaCl added (mM) denoted in the buffer name). All samples were prepared for western blot by boiling in 1× Laemmli buffer containing 0.1 M DTT.

Immunofluorescence. RWPE1;*LACZ* and RWPE1;SCHLAP1 cells were grown on 0.1% gelatin-coated glass coverslips, fixed in 2% paraformaldehyde, blocked in antibody dilution buffer (goat serum PBS), and immunostained for SMARCA4 (abcam, 1:500 dilution) and SMARCB1 (abcam, 1:400 dilution) overnight at 4 °C in antibody dilution buffer. Coverslips were washed three times for 5 min in PBS and then stained with secondary antibody (goat anti-rabbit, Alexa Fluor 568, 1:500 in antibody dilution buffer) for 45 min at 20–25 °C. Coverslips were again washed three times for min in PBS and mounted with Prolong Gold containing DAPI and imaged on a Zeiss Axio Imager 2.

Growth assays. Two-dimensional (2D) growth assays were performed by plating 1,000 cells per well in 96-well plates. Assays were carried out 1, 3, and 5 days post plating using Cell Titer Glo (Promega). Three-dimensional (3D) growth assays were performed by plating 10 or 100 cells per well in 96-well plates and counting cell growth using Cell Titer Glo 3D (Promega) 4 days after plating.

Immunoprecipitation. Nuclear lysates and co-immunoprecipitation were performed as described previously[4]. Cells were washed with PBS and then centrifuged at 1,300 rpm for 10 min at 4 °C. Cells were washed with 20 packed cell volumes of hypotonic cell lysis buffer (10 mM HEPES–KOH pH 7.9, 1.5 mM MgCl₂, 10 mM KCl, 0.5 mM DTT plus protease inhibitors) and placed on ice for 10 min to swell. Cells were then centrifuged at 1,300 rpm for 10 min at 4 °C. Cells were homogenized using a Dounce with a 'B' pestle in 2 packed cell volumes of hypotonic cell lysis buffer. Nuclei were pelleted at 1,300 rpm for 10 min at 4 °C, washed with 10 packed cell volumes of hypotonic cell lysis buffer, and centrifuged at 5,000 rpm for 10 min. Extractions were performed twice with 0.6 volume nuclear lysis buffer (20 mM HEPES–KOH pH 7.9, 25% glycerol, 420 mM KCl, 1.5 mM MgCl₂, 0.2 mM EDTA, 0.5 mM DTT, and protease inhibitors). Lysates were clarified at 14,000 rpm for 10 min at 4 °C between extractions. Lysates were

diluted with storage buffer (20 mM HEPES–KOH pH 7.9, 20% glycerol, 0.2 mM EDTA, 0.2 mM DTT) to bring the final KCl concentration to 150 mM, and stored at −80 °C.

Prior to beginning the immunoprecipitation, we washed protein A magnetic beads three times with PBS +0.5% BSA at 4 °C. We resuspended beads in 400 µl of 1× +0.5% BSA, then added 4–10 µg of antibody and incubated overnight at 4 °C. The following day, we thawed the nuclear lysates on ice. Lysates were added to antibody-conjugated beads and incubated overnight. Beads were washed four times with BC-150 (20 mM HEPES–KOH pH 7.9, 0.15 M KCL, 10% glycerol, 0.2 mM EDTA pH 8.0, 0.1% Tween-20, 0.5 mM DTT and protease inhibitors), two times with BC-100 (20 mM HEPES–KOH pH 7.9, 0.1 M KCL, 10% glycerol, 0.2 mM EDTA pH 8.0, 0.1% Tween-20, 0.5 mM DTT and protease inhibitors), and once with BC-60 (20 mM HEPES–KOH, pH 7.9, 60 mM KCl, 10% glycerol, 0.5 mM DTT and protease inhibitors). Proteins were eluted from beads using 2× Laemmli buffer with 100 mM DTT for 10 min at 95 °C.

ChIP–seq. ChIP experiments were performed as described previously[4]. Cells were fixed for 30 min at 4 °C in 0.3% methanol-free formaldehyde, quenched for 5 min with 125 mM glycine, washed three times, and snap frozen in liquid nitrogen and stored at −80 °C. Frozen pellets were thawed for 30 min on ice, resuspended each pellet in 1 ml swelling buffer (25 mM HEPES, 1.5 mM MgCl$_2$, 10 mM KCl, 0.1% IGEPAL CA-630 containing 1 mM PMSF and 1× protease inhibitor cocktail, Roche) and incubated 10 min at 4 °C. Cells were dounced 20 strokes with a 'B' pestle, and then nuclei were pelleted at 2,000 rpm for 7 min at 4 °C. The nuclei were washed with 10 ml MNase digestion buffer (15 mM HEPES pH 7.9, 60 mM KCl, 15 mM NaCl, 0.32 M sucrose) and pelleted at 2,000 rpm for 7 min at 4 °C. The pellet was then resuspended in 1 ml MNase digestion buffer per 4 × 10^7 cells, 3.3 µl 1 M CaCl$_2$ per ml, PMSF (1 mM) and protease inhibitor cocktail (1× , Roche) and then incubated for 5 min at 37 °C to warm. We added MNase (New England Biolabs M0247S 2,000 U µl^{-1}) at 0.5 µl per 1 × 10^7 cells and incubated for 15 min at 37 °C with agitation. Following digestion, the MNase was chelated using 1/50 volume 0.5 M EGTA on ice for 5 min. We added 1 volume of 2× IP buffer (20 mM TrisCl pH 8, 200 mM NaCl, 1 mM EDTA, 0.5 mM EGTA), then passed the sample through a 21-gauge needle five times and added Triton X-100 to 1% final concentration. The sample was cleared at 13,000 rpm for 15 min at 4 °C, and chromatin was incubated with antibody overnight at 4 °C (SMARCA4 (Abcam ab110641), SMARCA2 (Cell signaling 11966), SMARCB1 (Abcam)). Antibody–chromatin complexes were captured with protein A magnetic beads (Bio-Rad) for 2 h at 4 °C and washed five times with Agilent RIPA (50 mM HEPES pH 7.9, 500 mM LiCl, 1 mM EDTA, 1% IGEPAL CA-630, 0.7% Na-deoxycholate) and once with 10 mM Tris, 1 mM EDTA, 50 mM NaCl. DNA was eluted at 65 °C with agitation using 100 µl freshly made 1% SDS, 100 mM NaHCO$_3$. Crosslinks were reversed overnight by adding 5 µl of 5 M NaCl and incubating at 65 °C. DNA was treated with 3 µl RNaseA for 30 min at 37 °C and then proteinase K for 1 h at 56 °C and purified with Zymo Clean and Concentrator ChIP Kit and quantified using qubit before library preparation (Kapa Hyperprep).

ChIP–seq analysis. Reads were aligned to hg38 using bowtie2 (ref. [25]) using the sensitive parameters, and duplicates were removed using SAMtools[26]. For visualization, bigwig tracks were generated using DeepTools[27] (version 2.5.2), bamCoverage tool with a binsize of 30 bp and extending fragments to the

approximate nucleosome size of 150 bp. Tracks can be visualized using IGV[28], and bigwig files are available under GEO accession number GSE114392.

Peak calling. Peaks were called using Macs2 (version 2.1.0 (ref. [29])) using the narrowpeak mode and the following parameters: Qval = 0.05 –keep-dup-all --fix-bimodal –nomodel –extsize 150. In addition, we filtered the peaks against the ENCODE blacklist regions. Peaks were then annotated for the nearest transcription start site using ChIPPeakAnno[30] relative to GENCODE v26.

ATAC-seq. ATAC-seq was performed as described previously[10] but with modifications. In brief, 50,000 cells were collected and lysed in a buffer containing 0.05% IGEPAL CA-630 before transposition with a Nextera library prep kit containing TN5 transposomes. Libraries were amplified using 6–8 PCR cycles to enrich for TN5 products and add indexes and sequenced as paired-end 50-bp libraries on a HiSeq 2500. ATAC-seq data are available under GEO accession number GSE114391.

ATAC-seq analysis. Nextera adapter sequences were trimmed using trim_galore and reads were aligned to hg38 using bowtie2 with the -X 2000 setting[25]. We removed any reads mapping to the mitochondrial genome and filtered any reads with a mapping quality less than 20 using SAMtools[26]. Peaks were called using Macs2 (version 2.1.0 (ref. [29])) using the narrowpeak mode using default settings and --keep-dup-all. Differential openness was identified use csaw[31] with window size 150 and background window size 5,000, and an adjusted false discovery rate (FDR) of 0.05 for the combined windows. Motif analysis was performed using HOMER by comparing the open or closed ATAC sites to the background set of static sites[32].

Code availability. All commands, settings, or programs used to generate figures are described in the analysis section above. Any additional code used to generate figures is available upon reasonable request.

Reporting Summary. Further information on research design is available in the Nature Research Reporting Summary linked to this article.

Data availability
All data are available from GEO under accession number GSE114394. ATAC-seq and ChIP–seq read depth information can be found in Supplementary Table 7.

References
23. Méndez, J. & Stillman, B. *Mol. Cell. Biol.* **20**, 8602–8612 (2000).
24. Herrmann, C., Avgousti, D. C. & Weitzman, M. D. *Bio. Protoc.* **7**, e2175 (2017).
25. Langmead, B. & Salzberg, S. L. *Nat. Methods* **9**, 357–359 (2012).
26. Li, H. et al. *Bioinformatics* **25**, 2078–2079 (2009).
27. Ramírez, F. et al. *Nucleic Acids Res.* **44**, W160–W165 (2016).
28. Robinson, J. T. et al. *Nat. Biotechnol.* **29**, 24 (2011).
29. Zhang, Y. et al. *Genome. Biol.* **9**, R137 (2008).
30. Zhu, L. J. et al. *BMC Bioinformatics* **11**, 237 (2010).
31. Lun, A. T. L. & Smyth, G. K. *Nucleic Acids Res.* **44**, e45 (2016).
32. Heinz, S. et al. *Mol. Cell* **38**, 576–589 (2010).